

Crystallization and preliminary X-ray analysis of the molybdenum-dependent pyrogallol-phloroglucinol transhydroxylase of *Pelobacter acidigallici*Dietmar J. Abt,<sup>a</sup> Oliver Einsle,<sup>a,b</sup>  
Holger Niessen,<sup>a</sup>  
Robert Krieger,<sup>a</sup>  
Albrecht Messerschmidt,<sup>b</sup>  
Bernhard Schink<sup>a</sup> and  
Peter M. H. Kroneck<sup>a\*</sup><sup>a</sup>Universität Konstanz, Mathematisch-Naturwissenschaftliche Sektion, Fachbereich Biologie, Postfach M665, 78457 Konstanz, Germany, and <sup>b</sup>Max-Planck-Institut für Biochemie, Abteilung Strukturforschung, Am Klopferspitz 18a, 82152 Martinsried, GermanyCorrespondence e-mail:  
peter.kroneck@uni-konstanz.de

Crystals of the molybdo-iron-sulfur protein pyrogallol:phloroglucinol hydroxyltransferase (transhydroxylase; EC 1.97.1.2) from *Pelobacter acidigallici* were grown by vapour diffusion in an N<sub>2</sub>/H<sub>2</sub> atmosphere using polyethylene glycol as a precipitant. In this microorganism, transhydroxylase converts pyrogallol to phloroglucinol in a unique reaction without oxygen transfer from water. Growth of crystals suitable for X-ray analysis was strongly dependent on the presence of dithionite as a reducing agent. The crystals belonged to space group *P*1 and MAD data were collected on the iron *K* edge to resolutions higher than 2.5 Å.

Received 3 July 2001  
Accepted 28 November 2001

## 1. Introduction

Aerobic degradation of aromatic compounds involves oxygenase reactions in the primary attack on the mesomeric ring structure. In the absence of dioxygen, the stability of the aromatic nucleus is often overcome by a reductive attack (Evans, 1977; Reichenbecher *et al.*, 1994). Gallic acid is decarboxylated to pyrogallol and subsequently transformed to phloroglucinol in a unique reaction by transhydroxylase (Fig. 1). Although this hydroxyl transfer does not represent a net redox reaction, the substrate pyrogallol is oxidized in position 5 and the cosubstrate 1,2,3,5-tetrahydroxybenzene is reduced in position 2. Recently, it was shown by incubation with <sup>18</sup>OH<sub>2</sub> that there is no oxygen transfer from water in the transhydroxylase reaction and that the hydroxyl groups are transferred only between the phenolic substrates (Reichenbecher & Schink, 1999). Transhydroxylase differs fundamentally from all known hydroxylating molybdenum enzymes, which derive their hydroxyl groups from water. Phloroglucinol, the product of the transhydroxylase reaction, undergoes reductive dearomatization (Brune & Schink, 1990; Schink & Pfennig, 1982) and subsequent hydrolytic cleavage to 3-hydroxy-5 oxohexanoate, which is oxidized and thiolitically

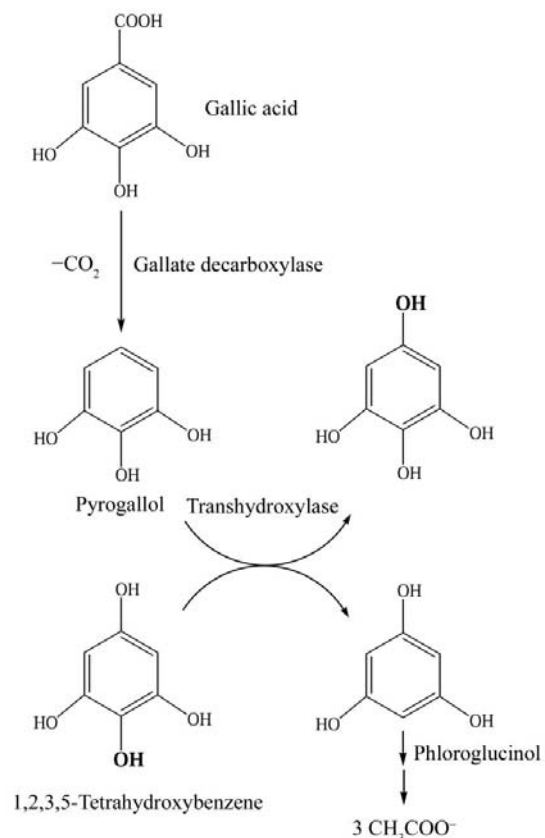


**Figure 1**  
Transhydroxylase reaction in the degradation pathway of gallic acid in *P. acidigallici* (Brune & Schink, 1992).

cleaved to three acetyl-CoA molecules (Brune & Schink, 1992).

According to its amino-acid sequence (Baas & Rétey, 1999; Reichenbecher *et al.*, 1996), transhydroxylase is a member of the DMSO

**Table 1**

Purification of *P. acidigallici* transhydroxylase from 34 g of cells; 1 U = 1  $\mu\text{mol}$  phloroglucinol  $\text{min}^{-1}$ .

Activities in parentheses are taken from (Reichenbecher *et al.*, 1994).

	Protein (mg)	Activity (U)	Specific activity (U $\text{mg}^{-1}$ )	Yield (protein) (%)	Yield (activity) (%)	Enrichment factor
Crude extract	3018	2417	0.80 (0.39)	100	100	1
DE-52	784	1501	1.92 (0.76)	26	62	2.4
Superdex	161	743	4.60 (3.10)	5	31	5.8

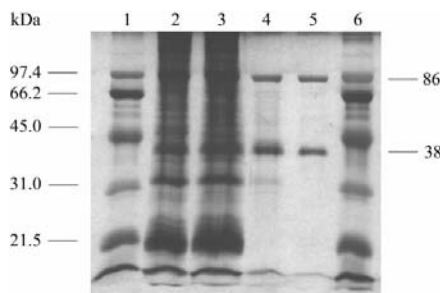


**Figure 2**

SDS-PAGE (12%) analysis of the transhydroxylase purification steps. Lanes 1 and 6, molecular-weight markers; lane 2, crude extract (6.2  $\mu\text{g}$  protein); lane 3, crude extract after ultrafiltration (5.8  $\mu\text{g}$ ); lane 4, transhydroxylase after DE-52 (2.9  $\mu\text{g}$ ); lane 5, transhydroxylase after Superdex (2.1  $\mu\text{g}$ ).



**Figure 3**

Crystals of transhydroxylase obtained by sitting-drop vapour diffusion in an  $\text{N}_2/\text{H}_2$  atmosphere.

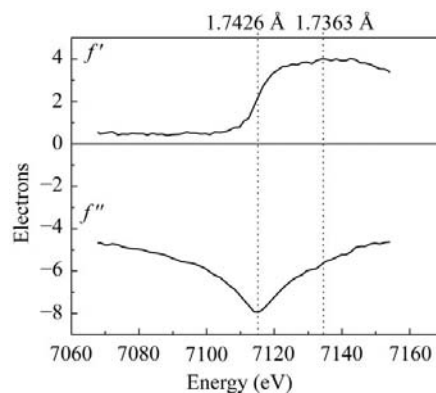


**Figure 4**

$f'$  and  $f''$  contributions derived from the fluorescence scan at the iron  $K$  edge according to the Kramers-Kronig transform. The  $f'$  and  $f''$  data sets were measured at the indicated wavelengths and a remote data set was collected at 1.05  $\text{\AA}$ .

reductase family of molybdoproteins and contains one molybdenum coordinated by two molybdopterin-guanidine dinucleotide cofactors in the large (100 kDa)  $\alpha$ -subunit and three [4Fe-4S] clusters in the small (31 kDa)  $\beta$ -subunit (Kisker *et al.*, 1999).

## 2. Materials and methods

### 2.1. Protein preparation

*P. acidigallici* strain Ma Gal 2 (DSM 2377) was grown anaerobically in a sulfide-reduced and bicarbonate-buffered saltwater mineral medium, as described previously (Brune & Schink, 1990). The substrate gallic acid was fed initially to 7 mM and twice (to 7 mM) during cultivation.

Transhydroxylase was prepared in the presence of air at 278 K according to Reichenbecher *et al.* (1994), omitting the chromatofocussing step.

### 2.2. X-ray analysis

Diffraction experiments were carried out on beamline BW6 at DESY, Hamburg using tunable synchrotron radiation. Data were integrated and scaled using the *HKL* suite (Otwinowski & Minor, 1996). Self-rotation functions were calculated with *GLRF* (Tong & Rossmann, 1990).

## 3. Results and discussion

### 3.1. Protein preparation

In order to obtain well diffracting crystals of the transhydroxylase, a modified purification scheme had to be developed. This led to a highly active (Table 1) and electrophoretically pure (Fig. 2) heterodimer, as previously reported (Reichenbecher *et al.*, 1994). Baas & Rétey (1999) reported a molecular mass of 99 260.3 Da for the  $\alpha$ -subunit and one of 31 331.2 Da for the  $\beta$ -subunit (total excluding cofactors: 130 481.5 Da), based on amino-acid sequence analysis.

### 3.2. Crystallization

Initial crystals of *P. acidigallici* transhydroxylase were obtained by sitting-drop vapour diffusion from Crystal Screen solution 42 (Hampton Research, Laguna Niguel, USA) under  $\text{N}_2/\text{H}_2$  and the preparations were stored in a desiccator at 293 K. Large trigonal prisms grew within 3 d from 12  $\text{mg ml}^{-1}$  protein reduced with a 12-fold excess of sodium dithionite. The crystals were optimized with solution 7 as additive (Fig. 3).

25% of methylpentanediol was added as cryoprotectant and the crystals were flash-cooled in the nitrogen stream of an Oxford cryosystem. It was possible to increase the diffraction limit of the crystals and at the same time decrease their mosaic spread through humidity control (Kiefersauer *et al.*, 2000). After this transformation, however, the crystals could no longer be flash-cooled and deteriorated quickly in the X-ray beam. Data sets were therefore collected from a non-transformed crystal at 100 K.

### 3.3. Data collection

The crystal used for the MAD experiment had dimensions of approximately  $500 \times 300 \times 50 \mu\text{m}$  and diffracted to a resolution of around 2  $\text{\AA}$ . Three full data sets were collected at a wavelength of 1.7363  $\text{\AA}$  to maximize the anomalous  $f''$  contribution, at 1.7426  $\text{\AA}$  for the  $f'$  inflection and a remote data set at 1.05  $\text{\AA}$  (Fig. 4). All data sets were integrated to a maximum resolution of 2.35  $\text{\AA}$ .

The crystal belonged to space group  $P1$ , with unit-cell parameters  $a = 173.2$ ,  $b = 179.1$ ,  $c = 180.5 \text{\AA}$ ,  $\alpha = 63.8$ ,  $\beta = 64.1$ ,  $\gamma = 65.0^\circ$ . The asymmetric unit could accommodate 12

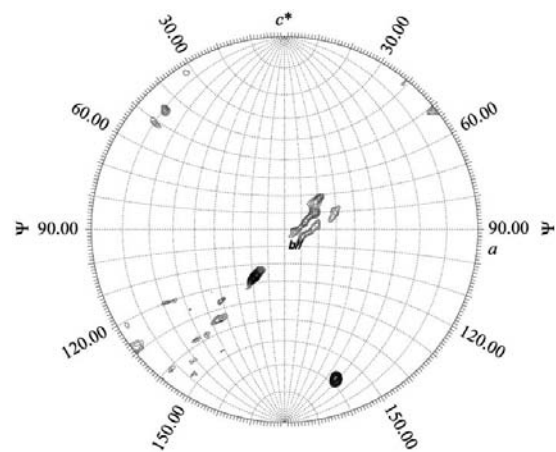


**Figure 5**

Polar plot of a self-rotation function for  $\kappa = 180^\circ$  (twofold correlation). Two twofold axes can clearly be seen at  $\Phi = 109^\circ$ ,  $\Psi = 117^\circ$  and  $\Phi = 31^\circ$ ,  $\Psi = 158^\circ$ .

heterodimers of transhydroxylase with a Matthews coefficient of  $2.71 \text{ \AA}^3 \text{ Da}^{-1}$ , corresponding to a solvent content of 55%. The structure solution in *P1* has to describe a total molecular mass of 1.6 MDa, containing 144 Fe atoms in 36 clusters plus 12 Mb atoms. A self-rotation function calculated in *P1* (Fig. 5) shows two clear twofold axes and a splitting of a further twofold axis into three parts.

The authors would like to thank Gleb P. Bourenkov, MPG-ASMB, DESY Hamburg

for help with MAD data collection.

## References

- Baas, D. & Rétey, J. (1999). *Eur. J. Biochem.* **265**, 896–901.
- Brune, A. & Schink, B. (1990). *J. Bacteriol.* **172**, 1070–1076.
- Brune, A. & Schink, B. (1992). *Arch. Microbiol.* **157**, 417–424.
- Evans, W. C. (1977). *Nature (London)*, **270**, 17–22.
- Kiefersauer, R., Than, M. E., Dobbek, H., Gremer, L., Melero, M., Strobl, S., Dias, J. M., Soulimane, T. & Huber, R. (2000). *J. Appl. Cryst.* **33**, 1223–1230.
- Kisker, C., Schindelin, H., Baas, D., Rétey, J., Meckenstock, U. R. & Kroneck, P. M. H. (1999). *FEMS Microbiol. Rev.* **22**, 503–521.
- Otwinowski, Z. & Minor, W. (1996). *Methods Enzymol.* **276**, 307–326.
- Reichenbecher, W., Brune, A. & Schink, B. (1994). *Biochim. Biophys. Acta*, **1204**, 217–224.
- Reichenbecher, W., Rüdiger, A., Kroneck, P. M. H. & Schink, B. (1996). *Eur. J. Biochem.* **237**, 406–413.
- Reichenbecher, W. & Schink, B. (1999). *Biochim. Biophys. Acta*, **19**, 245–253.
- Schink, B. & Pfennig, N. (1982). *Arch. Microbiol.* **133**, 195–201.
- Tong, L. & Rossmann, M. G. (1990). *Acta Cryst.* **A46**, 783–792.